

# Search and localization dynamics of the CRISPR/Cas9 system

Qiao Lu (路桥)<sup>1</sup>, Deepak Bhat<sup>1</sup>, Darya Stepanenko<sup>1,2,3</sup>, and Simone Pigolotti<sup>1\*</sup>

<sup>1</sup>*Biological Complexity Unit, Okinawa Institute of Science and Technology Graduate University, Onna, Okinawa 904-0495, Japan,*

<sup>2</sup>*Lauffer Center for Physical and Quantitative Biology, Stony Brook University, New York, USA, and*

<sup>3</sup>*Department of Applied Mathematics and Statistics, Stony Brook University, New York, USA.*

(Dated: August 23, 2021)

The CRISPR/Cas9 system acts as the prokariotic immune system and has important applications in gene editing. The protein Cas9 is a crucial component of this system. The role of Cas9 is to search for specific target sequences on the DNA and cleave them. In this Letter, we show that a model of facilitated diffusion fits data from single-molecule experiments and predicts that Cas9 search for targets by sliding, but with a short sliding length. We then investigate how Cas9 explores a long DNA containing randomly placed targets. We solve this problem by mapping it into the theory of Anderson localization in condensed matter physics. Our theoretical approach rationalizes experimental evidences on the distribution of Cas9 molecules along the DNA.

The discovery of the CRISPR/Cas9 system has revealed the functioning of the bacterial immune system and, at the same time, has opened previously unimaginable possibilities for gene editing [1]. The protein Cas9 is a central actor in this system. Cas9 is an endonuclease that is able to load a guide RNA strand. Its target is a sequence on the DNA complementary to the guide RNA, which Cas9 can identify and cleave. This recognition process has attracted considerable attention, including from the modeling side [2–4]. Recognition is triggered by a three-base sequence called protospacer adjacent motif (PAM), which precedes the target. The first two bases of a PAM are guanine, whereas the third can be any base. Cas9 can transiently bind to a PAM even in the absence of a neighboring target [5, 6].

Other proteins such as the Lac repressor in *Escherichia coli* [7] find their targets along the DNA by a mechanism termed facilitated diffusion – an alternance of 3D diffusion in the cytosol and one-dimensional diffusive sliding along the DNA chain [8]. This mechanism can significantly improve search efficiency [8, 9]. The theory of facilitated diffusion has been extended to take into account the energetics of target search along the DNA [10–12] and to include other processes such as hopping, i.e., the possibility for proteins to briefly detach from DNA and then reattach at short distance [13]. This body of work has naturally lead to the hypothesis that Cas9 finds its target using facilitated diffusion as well.

However, experimental single-molecule studies using DNA curtains [14] and fluorescence resonance energy transfer (FRET) [15] did not find evidences of sliding. They however found that the lifetime of Cas9 binding events is well fitted by a double exponential even in the absence of targets, suggesting a complex binding mechanisms. In contrast, a more recent FRET experimental study suggests that Cas9 can slide [6]. This study found that, in a DNA sequence containing multiple PAMs without targets, the two exponential constants characterizing the binding lifetime distribution depend on the number

of PAMs and the distance between them. In the absence of PAMs, this distribution reduces to a single exponential. The dependence of the exponential constants on the distance between PAMs suggest that the characteristic sliding length of Cas9 falls below the spatial resolution of previous experiments [14], potentially explaining why sliding was not previously observed.

An alternative way of probing the search dynamics of Cas9 is provided by immunoprecipitation experiments [16]. These experiments permit to estimate the distribution of Cas9 molecules bound along the DNA. They reveal that Cas9 is localized in regions that extend for about 200 base pairs length around targets [16–19]. This length scale is much larger than the sliding length suggested by the experiments in Ref. [6].

These contrasting experimental evidences call for a theoretical explanation. To this aim, it is useful to think about a bacterial genome as a long stretch of DNA in which a large number of PAMs are disorderly distributed. For comparison, the *E.coli* genome is 4.6 million base pairs long and contains about half million PAMs [5]. We focus on the typical localization length associated with the dynamics of Cas9 on such DNA sequences. This problem bears an analogy with the theory of Anderson localization [20]. This theory predicts that, under general conditions, eigenvectors of disordered one-dimensional diffusive systems are localized, with profound consequences for fields of physics ranging from condensed matter to disordered and chaotic systems [21]. In this analogy, PAMs play the role of defects in one dimensional lattices.

In this Letter, we show that a facilitated diffusion model quantitatively explains the dynamics of Cas9 observed in single-molecule experiments. We then explore the analogy with Anderson localization to determine the localization length of Cas9 on typical long DNA strands.

We consider a Cas9 protein that binds on a DNA chain of length  $N$  and slides along it before detaching, see Fig. 1. Our aim is to quantify the distribution of duration of binding events depending on the arrangement

of specific PAM sites along the DNA chain. We introduce the probability  $p_n(t)$  that Cas9 is bound at site  $n$  at time  $t$ , given that it had attached on the DNA at time  $t = 0$ . Each site represents a nucleotide position  $n = 1 \dots N$ . We assume attachment to be non specific, so that  $p_n(t = 0) = 1/N$ .

We distinguish between two types of DNA sites. PAM sites are those at the beginning of a PAM sequence, where Cas9 can bind specifically. We consider every other site as non-specific, including the two other base pairs constituting a PAM, see Fig. 1. We call  $E_n$  the binding energy of Cas9 at position  $n$ . We assume that all non-specific sites have the same binding energy  $E_n = 0$ . If  $n$  is a PAM site, then  $E_n = -\beta$ , with  $\beta > 0$ . All energies are expressed in units of  $k_B T$ , where  $k_B$  is the Boltzmann constant and  $T$  the temperature. Our aim is to analyze single binding events and therefore we do not consider rebinding after detachment.

The probabilities  $p_n(t)$  evolve according to the master equation

$$\frac{d}{dt}p_n(t) = D_{n,n+1}p_{n+1} + D_{n,n-1}p_{n-1} - (D_{n+1,n} + D_{n-1,n} + k_n)p_n, \quad (1)$$

in which  $D_{n,m} = D e^{E_m}$  and  $k_n = k e^{E_n}$ , where  $D$  and  $k$  are given parameters. We impose vanishing fluxes at the boundaries,  $D_{0,1} = D_{1,0} = D_{N,N+1} = D_{N+1,N} = 0$ . This choice of rates satisfies the detailed balance condition  $D_{n,m} e^{-E_m} = D_{m,n} e^{-E_n}$ .

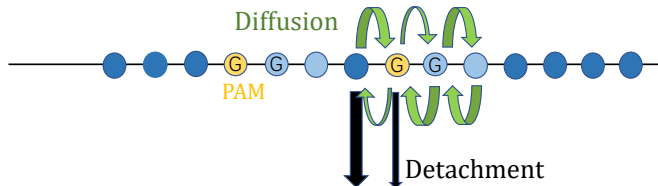


FIG. 1: Scheme of the model. PAM sites and non-specific sites are shown in yellow and blue, respectively. The second and third bases of PAM sequences are considered as non-specific sites (light blue). Green arrows represent sliding rates and black arrows represent detachment rates, see Eq. (2). Thicker arrows correspond to larger rates.

We express the model in vector notation by defining  $\mathbf{p}(t) = (p_1(t), p_2(t) \dots p_N(t))$ . We write Eq. (1) as  $d\mathbf{p}/dt = \hat{A}\mathbf{p}$ , where the elements  $A_{m,n}$  of the matrix  $\hat{A}$  are given by

$$A_{m,n} = \begin{cases} D e^{E_n} & \text{if } |n - m| = 1 \\ -(k + 2D) e^{E_m} & \text{if } n = m. \end{cases} \quad (2)$$

The formal solution to the master equation is  $\mathbf{p}(t) = e^{\hat{A}t} \mathbf{p}(0)$ , where  $\mathbf{p}(0)$  is the uniform initial condition. For later convenience, we introduce the eigenvalue equation associated with the master equation:

$$\hat{A}\boldsymbol{\psi} = -\lambda\boldsymbol{\psi}. \quad (3)$$

Equation (3) is solved by a set of eigenvalues  $\lambda = \lambda_1, \lambda_2, \dots, \lambda_N$  and associated right eigenvectors  $\boldsymbol{\psi} = \boldsymbol{\psi}^{(1)}, \boldsymbol{\psi}^{(2)}, \dots, \boldsymbol{\psi}^{(N)}$ , assumed to be normalized. The solution of the master equation can be decomposed into eigenvalues

$$\mathbf{p}(t) = \sum_{i=1}^N e^{-\lambda_i t} c_i \boldsymbol{\psi}^{(i)}, \quad (4)$$

where the  $c_i$  are coefficients determined by the initial condition. Because of detachment, one has  $\lim_{t \rightarrow \infty} p_i(t) = 0$  for all  $i$ . This fact and the detailed balance condition imply that all eigenvalues must be real and positive. We sort the eigenvalues so that  $\lambda_1$  is the smallest one.

The total probability that Cas9 is still bound at a time  $t$  is given by  $P(t) = \sum_n p_n(t)$ . Since we are considering a single binding event,  $P(t)$  is a decreasing function of  $t$ . We define the instantaneous detachment rate  $g(t) = -d/dt P(t)$ . Single-molecule experiments [6, 14, 15] have found that the temporal decay of  $g(t)$ , and therefore of  $P(t)$ , is characterized by two distinct exponential slopes at short and long times.

To understand these two regimes, we focus on  $P(t)$  and define its instantaneous exponential slope  $K(t) = -d/dt \ln P(t)$ . We also define the total probability  $P_{\text{PAM}}(t) = [\sum_{n \in \text{PAM}} p_n(t)]/P(t)$  of Cas9 being bound to a PAM site at time  $t$ , given that it had not detached yet. By summing Eq. (1) over  $n$ , we find that

$$K(t) = k [1 - P_{\text{PAM}}(t)] + k e^{-\beta} P_{\text{PAM}}(t). \quad (5)$$

Considering that  $0 \leq P_{\text{PAM}}(t) \leq 1$ , the slope  $K(t)$  is limited by the two detachment rates:

$$k e^{-\beta} \leq K(t) \leq k. \quad (6)$$

The value of  $K(t)$  in this range is determined by  $P_{\text{PAM}}(t)$ . Since the initial distribution is uniform, at short times  $P_{\text{PAM}}$  is simply equal to the fraction of PAM sites. Given that this fraction is usually small, Eq. (5) implies  $K(t) \approx k$  at short times. In contrast, the eigenvector expansion of Eq. (4) leads to conclude that the exponential slope in the long time limit should be  $K(t) = \lambda_1$ .

Experiments in [6] measured the distribution of Cas9 binding events on different DNA sequences, containing from 0 to 5 PAM sequences. We jointly fitted the parameters  $k$ ,  $\beta$ , and  $D$  to these six experiments, see Fig. 2a. Solutions of the master equation (1) with the best-fit parameters reproduce the double exponential behavior and fit well the experimental data, see Fig. 2b. At increasing number of PAM sites, the second slope becomes significantly less steep than the first. According to Eq. (5), this means that, at long times, Cas9 is much more localized on PAM sites compared with short times. Inspecting the eigenvectors  $\boldsymbol{\psi}^{(1)}$  associated with the smallest eigenvalue  $\lambda_1$  confirms this idea, see Fig. 2c.

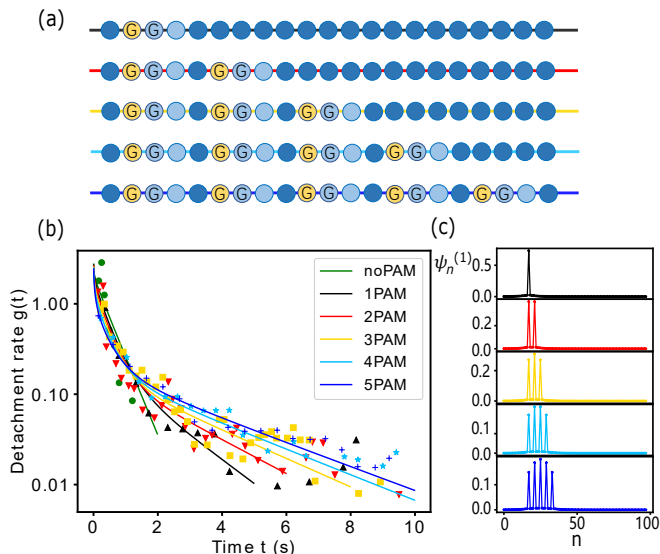


FIG. 2: (a) Arrangements of PAM sites used in the experiments in [6]. The line colors correspond to the different curves in panel b. The figure shows only the portion of the DNA sequence of length  $N = 98$  where the PAM sites are located. (b) Comparison of the prediction of our model (lines) with experiments [6] (points). To fit the data, we express the likelihood as  $\mathcal{L}_j = \prod_i [\mathcal{N}_j! \rho_{i,j}^{n_{i,j}} / n_{i,j}!]$ , where the index  $0 \leq j \leq 5$  indicates the number of PAM sites in each experiment. For each experiment  $j$ ,  $n_{i,j}$  is the number of binding events in the  $i$ th bin of the histogram,  $\mathcal{N}_j$  is the total number of binding events, and  $\rho_{i,j} = P(t_{i-1}) - P(t_i)$  is the probability of an event of duration falling into the  $i$ th bin. This probability is obtained from numerical integration of Eq. (1) for a given choice of the parameters  $k$ ,  $D$ , and  $\beta$ , with a matrix  $\hat{A}$  determined by the arrangement of PAM sites in the given experiment. We maximize the joint log-likelihood  $\sum_{j=0}^5 \ln \mathcal{L}_j$  with respect to the three parameters and compute their uncertainties from the curvature of the log-likelihood. The best-fit parameters are  $k = 1.94 \pm 0.10 \text{ s}^{-1}$ ,  $\beta = 3.34 \pm 0.07$ , and  $D = 52 \pm 9 \text{ bp}^2 \text{ s}^{-1}$ . (c) Eigenvectors  $\psi^{(1)}$  for  $j = 1 \dots 5$ .

To gain further insight into the dynamics observed in Fig. 2b, we analytically compute  $\lambda_1$  and its eigenvector for an infinitely long chain with a single PAM site at position  $n = 0$ . For  $|n| > 1$ , the eigenvector must satisfy

$$-\lambda_1 \psi_n^{(1)} = D \left( \psi_{n+1}^{(1)} + \psi_{n-1}^{(1)} - 2\psi_n^{(1)} \right) - k\psi_n^{(1)}. \quad (7)$$

We assume a solution of the form  $\psi_n \propto e^{-|n|/\ell}$  where  $|n| > 0$  and we define  $\ell$  as the sliding length. Substituting this expression into Eq. (7) we obtain

$$k - \lambda_1 = 2D[\cosh(1/\ell) - 1] \quad (8)$$

By expanding the cosh at first order we find  $\ell \approx \sqrt{D/(k - \lambda_1)}$ . Note that  $\lambda_1 \leq k$  due to Eq. (6). The three unknown  $\lambda_1$ ,  $\ell$  and  $\psi_0$  can be determined from Eq. (8) and the equivalents of Eq. (7) for  $n = 0$  and  $|n| = 1$ . Substituting the fitted parameters of Fig. 2, we find the sliding length  $\ell \approx 6.2 \text{ bp}$ .

Both our model and experiments [6] show that the lifetime of long binding events increases at increasing number of PAMs, see Fig. 2b. In the model, this means that  $\lambda_1$  is a decreasing function of the number of PAMs. This effect can be explained by interference among PAM sites. To show that, we consider a finite number of equispaced PAM sites on an infinite DNA chain. If the distance between the PAM sites is much larger than the sliding length  $\ell$ , then binding events around each PAM site would behave independently. It follows that, in this limit, the exponential slope at long times must be the same as in the case of a single PAM site, regardless of the number of PAM sequences. This prediction is confirmed by numerical simulations, see Fig. 3. As the distance between the PAM sites is reduced, interference leads to an increase in the occupancy of targets. This implies that, at large  $t$ ,  $P_{\text{PAM}}(t)$ , and therefore the lifetime of binding events, are decreasing functions of the interval between the PAM sites, see Eq. (5). Both these predictions are supported by a numerical computation of  $\lambda_1$  as a function of the interval between the PAM sites, see Fig. 3.

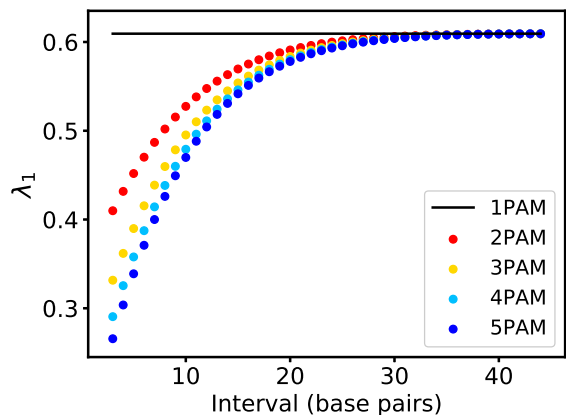


FIG. 3: Interference between PAM sequences. Lowest eigenvalue  $\lambda_1$  as a function of the separation between PAMs, for different number of PAM sequences. The results are obtained by numerically diagonalizing the matrix  $\hat{A}$  corresponding to each case, with  $N = 220$ . The horizontal line shows the value of  $\lambda_1$  for a DNA chain containing a single PAM sequence, from the exact solution of Eq. (7).

In summary, we found that the distribution of a Cas9 molecule in a small region of DNA containing several PAM sequences tends to be localized. We now study the behavior of Cas9 on a very long stretch of DNA including a disordered assortment of PAM sites. The theory of Anderson localization predicts that, in such disordered one-dimensional systems, eigenvectors are exponentially localized:

$$\psi_n \sim e^{-\frac{|n-n^*|}{\gamma(\lambda)}}, \quad (9)$$

where  $n^*$  is the location of the eigenvector peak and  $\gamma(\lambda)$  is the localization length associated with the eigenvalue

$\lambda$ . Our hypothesis is that the localization length associated with the smallest eigenvalues of Cas9 dynamics can explain the results of immunoprecipitation experiments.

We sharpen the analogy between our problem and the Anderson localization by rescaling the components of our eigenvectors by the Boltzmann weight,  $f_n = \psi_n \exp(E_n)$ . With this transformation, Eq. (3) assumes the same form for PAM and non-PAM sites:

$$f_{n+1} + f_{n-1} - \left(2 + \frac{k - \lambda e^{-E_n}}{D}\right) f_n = 0. \quad (10)$$

This equation is formally similar to the discrete Schrödinger equation in Anderson's original work [20]. It can be solved by the transfer matrix method. We introduce the vector  $\mathbf{f}_n = (f_n, f_{n-1})$  and the transfer matrix

$$\hat{T}_n = \begin{pmatrix} 2 + \frac{k - \lambda e^{-E_n}}{D} & -1 \\ 1 & 0 \end{pmatrix}. \quad (11)$$

With these definitions, we rewrite Eq. (10) as

$$\mathbf{f}_{n+1} = \hat{T}_n \mathbf{f}_n \quad (12)$$

and therefore

$$\mathbf{f}_N = \prod_{n=1}^{N-1} \hat{T}_n \mathbf{f}_1. \quad (13)$$

We assume that, in a typical long DNA sequence, each site  $n$  has a probability  $1/16$  to be a PAM site, thereby affecting the value of  $E_n$  in the corresponding matrix  $T_n$ . In this view, Eq. (13) expresses the solution of the eigenvalue equation as a product of random matrices [21].

The localization length  $\gamma$  can be calculated from this product by means of an approach proposed by Herbert, Jones, and Thouless [22, 23]. This approach rests on the idea that  $f_N(\lambda)$ , with appropriate boundary conditions, vanishes if  $\lambda$  is an eigenvalue. Moreover,  $f_N(\lambda)$  as a function of  $\lambda$  changes sign at every eigenvalue. This argument implies the expression

$$\frac{1}{N} \ln f_N(\lambda) = \frac{1}{N} \sum_{n=1}^{N-1} \ln |\lambda_n - \lambda| + \frac{i\pi}{N} \sum_{n=1}^{N-1} \theta(\lambda - \lambda_n) + \frac{1}{N} \ln A \quad (14)$$

where  $\theta$  is the Heaviside step function and  $A$  is a finite constant. Taking the limit  $N \rightarrow \infty$ , we define

$$\Lambda(\lambda) = \lim_{N \rightarrow \infty} \frac{1}{N} \ln f_N(\lambda) = \lim_{N \rightarrow \infty} \frac{1}{N} \ln \left( \text{Tr} \prod_{n=1}^N \hat{T}_n \right), \quad (15)$$

where in the second equality we substituted Eq. (13). The Furstenberg theorem guarantees that  $\Lambda(\lambda)$  is independent of the realization of the disorder and of the choice of  $\mathbf{f}_1$  [24, 25].

The inverse of the real part of  $\Lambda(\lambda)$  can be identified with the localization length  $\gamma(\lambda)$  thanks to a result

known as the Borland conjecture [26]. The validity of this conjecture for our class of systems is supported by numerical and theoretical studies [24, 27]. Further, because of Eq. (14), the imaginary part of  $\Lambda$  is proportional to the cumulative density of states. We calculate numerically both of these quantities using the transfer matrix, see Fig. 4. We find that the localization length for the whole spectrum is always shorter than 11 base pairs, much shorter than the localization length observed in immunoprecipitation experiments [16–19].

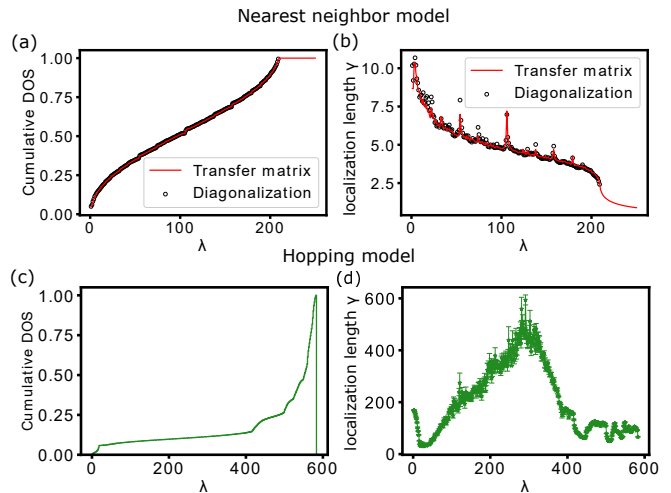


FIG. 4: (a) Cumulative density of states (DOS) and (b) localization length as function of  $\lambda$  for the nearest neighbour model, Eq. (1), computed using Eq. (14). Results obtained by the transfer matrix and by a direct diagonalization agree with each other. The DNA chain length is  $N = 10^6$  for the transfer matrix method and  $N = 5000$  for the direct diagonalization. (c) Cumulative DOS and (d) localization length for the hopping model expressed by Eq. (16), computed using Eq. (17). We estimate the hopping distribution from the solution of a diffusion equation in cylindrical coordinates [13], that leads to the expression  $W(q) = [1 + 2\pi\alpha|q|rK_1(|q|r)/(K_0(|q|r))]^{-1}$  for the Fourier transform of  $h(n)$ . Here,  $r = 3$  is the DNA radius, measured in unit of the base pair distance,  $K_n(x)$  is the modified Bessel function of the second kind, and  $\alpha = 1$  is the ratio between the 3D diffusion coefficient and the non-specific binding rate. We found qualitatively similar results for  $\alpha$  in the range  $0.1$  to  $10^5$  (not shown). For  $n > 1$ , we compute  $h(n)$  by a numerical inverse Fourier transform of  $W(q)$ . We truncate  $h(n)$  at a distance  $n_{\max} = 17$  for computational convenience. In this case, the DNA chain length is  $N = 2000$ .

We assume that this discrepancy is caused by a fundamental difference between immunoprecipitation and single-molecule experiments. Immunoprecipitation experiments provide an “ensemble average” which is potentially affected by search mechanisms other than sliding (such as hopping). In contrast, single-molecule FRET experiments measure single sliding events, which are unaffected by such mechanisms.

To test this idea, we generalize our model to include hopping. In a hopping event, Cas9 detaches and then

reattaches to the DNA at a short distance. This amounts to include in our master equation diffusion among non-nearest neighboring sites:

$$D_{m,n} = De^{E_n} h(|n - m|), \quad (16)$$

where  $h(n)$  is a positive decreasing function characterizing the probability of hopping events at a given distance  $n$  relative to sliding events. We impose  $h(1) = 1$ , so that nearest-neighbor sliding is consistent with Eq. (2). Detachment rates in the hopping model are the same as in Eq. (2). For models with next to nearest neighbor interactions, such as our hopping model, the localization length can not be computed using Eqs. (14) and (15), see [28]. We therefore estimate the localization length by a more direct strategy, although computationally heavier. Assuming that a given eigenvector  $\psi$  is localized, we obtain from Eq. (9) that

$$\gamma \sim -\frac{(N-1)}{\ln(\psi_1\psi_N)} \quad (17)$$

In this case, we find that the localization length associated with the lowest eigenvalues is on the order of 100 to 200 base pairs, see Fig. 4d, in agreement with immunoprecipitation experiments.

In conclusion, in this Letter we studied the search dynamics of Cas9 along the DNA. We have shown that the predictions of a facilitated diffusion model with a short sliding length are consistent with the result of single-molecule FRET experiments. By applying the theory of Anderson localization, we have argued that a hopping mechanism can explain how Cas9 is generically distributed along the DNA. Our approach can be generalized to more detailed models of Cas9 dynamics, including multiple conformations and binding to target sequences.

More in general, the analogy between facilitated diffusion and localization in disordered potentials explored in this Letter can be applied to other proteins, such as transcription factors binding to several weak targets on the DNA, to understand how different search mechanisms contribute to localize them.

---

\* Electronic address: simone.pigolotti@oist.jp

- [1] M. Jinek, K. Chylinski, I. Fonfara, M. Hauer, J. A. Doudna, and E. Charpentier, *Science* **337**, 816 (2012).  
 [2] I. Farasat and H. M. Salis, *PLoS Comput. Biol.* **12**, e1004724 (2016).

- [3] A. A. Shvets and A. B. Kolomeisky, *Biophys. J.* **113**, 1416 (2017).  
 [4] M. Klein, B. Eslami-Mossallam, D. G. Arroyo, and M. Depken, *Cell Rep.* **22**, 1413 (2018).  
 [5] D. L. Jones, P. Leroy, C. Unoson, D. Fange, V. Čurić, M. J. Lawson, and J. Elf, *Science* **357**, 1420 (2017).  
 [6] V. Globyte, S. H. Lee, T. Bae, J.-S. Kim, and C. Joo, *The EMBO J.* **38** (2019).  
 [7] P. Hammar, P. Leroy, A. Mahmutovic, E. G. Marklund, O. G. Berg, and J. Elf, *Science* **336**, 1595 (2012).  
 [8] O. G. Berg, R. B. Winter, and P. H. von Hippel, *Biochemistry* **24**, 6929 (1981).  
 [9] L. Mirny, M. Slutsky, Z. Wunderlich, A. Tafvizi, J. Leith, and A. Kosmrlj, *J. Phys. A: Math. Theor.* **42**, 434013 (2009).  
 [10] M. Slutsky and L. A. Mirny, *Biophys. J.* **87**, 4021 (2004).  
 [11] M. Bauer, E. S. Rasmussen, M. A. Lomholt, and R. Metzler, *Sci. Rep.* **5**, 1 (2015).  
 [12] M. Cencini and S. Pigolotti, *Nucleic Acids Res.* **46**, 558 (2018).  
 [13] M. A. Lomholt, B. van den Broek, S.-M. J. Kalisch, G. J. Wuite, and R. Metzler, *Proc. Natl. Acad. Sci.* **106**, 8204 (2009).  
 [14] S. H. Sternberg, S. Redding, M. Jinek, E. C. Greene, and J. A. Doudna, *Nature* **507**, 62 (2014).  
 [15] D. Singh, S. H. Sternberg, J. Fei, J. A. Doudna, and T. Ha, *Nat. Commun.* **7**, 1 (2016).  
 [16] C. Kuscus, S. Arslan, R. Singh, J. Thorpe, and M. Adli, *Nat. Biotechnol.* **32**, 677 (2014).  
 [17] R. Cencic, H. Miura, A. Malina, F. Robert, S. Ethier, T. M. Schmeing, J. Dostie, and J. Pelletier, *PloS one* **9**, e109213 (2014).  
 [18] Y. Gao, H. Wu, Y. Wang, X. Liu, L. Chen, Q. Li, C. Cui, X. Liu, J. e. Zhang, and Y. Zhang, *Genome Biol.* **18**, 1 (2017).  
 [19] C. Li, C. Chen, H. Chen, S. Wang, X. Chen, and Y. Cui, *Plant Biotechnol. J.* **16**, 1446 (2018).  
 [20] P. W. Anderson, *Phys. Rev.* **109**, 1492 (1958).  
 [21] A. Crisanti, G. Paladin, and A. Vulpiani, *Products of Random Matrices in Statistical Physics*, vol. 104 (Springer Science & Business Media, 2012).  
 [22] D. Herbert and R. Jones, *J. Phys. C: Solid State Phys.* **4**, 1145 (1971).  
 [23] D. Thouless, *J. Phys. C: Solid State Phys.* **5**, 77 (1972).  
 [24] K. Ishii, *Prog. Theor. Phys. Suppl.* **53**, 77 (1973).  
 [25] H. Furstenberg, *Trans. Am. Math. Soc.* **108**, 377 (1963).  
 [26] R. Borland, *Proc. R. Soc. London, Ser. A* **274**, 529 (1963).  
 [27] H. Matsuda and K. Ishii, *Prog. Theor. Phys. Suppl.* **45**, 56 (1970).  
 [28] J. Biddle, D. J. Priour Jr, B. Wang, and S. D. Sarma, *Phys. Rev. B* **83**, 075105 (2011).